Regular Article

PHYSICAL CHEMISTRY RESEARCH
Published by the
Iranian Chemical Society
www.physchemres.org
info@physchemres.org

***Phys. Chem. Res.**, Vol. 7, No. 1, 131-148, March 2019*
DOI: 10.22036/pcr.2018.152521.1548

Response Surface Methodology for Optimizing Adsorption Process Parameters of Amaranth Removal Using Magnetic Layer Double Hydroxide (Fe_3O_4/ZnFe-LDH)

N. Sohrabi*, N. Rasouli and F. Alirezaarab
Department of Chemistry, Payame Noor University, P. O. Box: 19395-3697, Tehran, Iran
(Received 18 October 2018, Accepted 19 December 2018)

Response surface methodology was employed to optimize the adsorption parameters of Amaranth onto magnetic layer double hydroxide (Fe_3O_4/ZnFe-LDH). Such optimization was undertaken to ensure a high efficiency over the experimental ranges employed, and to evaluate the interactive effects of the initial concentration of Amaranth, pH, adsorbent dosage, temperature and contact time on the adsorption process in order to improve the conditions employed in the batch process. A total of 32 desorption experimental runs were carried out employing the detailed conditions designed by response surface methodology based on the Box-Behnken design. The analysis of variance (ANOVA) indicated that a second-order polynomial regression equation was the most appropriate polynomial for fitting the experimental data. The experimental confirmation tests showed a correlation between the predicted and experimental responses (R^2). The optimal point obtained was located in the valid region and the optimum adsorption parameters were predicted as an initial Amaranth concentration of 70.93 mg l^{-1}, a pH value of 3.6, the adsorbent dosage of 0.01 g, a temperature of 31.82 °C and contact time of 16.83 min.

Keywords: Response surface, Adsorption, Amaranth, Magnetic layer double hydroxide

INTRODUCTION

Removing dyes from wastewater is a current issue for foundational research and practical application [1]. Dye contamination in industrial wastewater, resulted from paper, textiles, plastics, printing, leather and so on, has become the main concern because of their adverse effects on several forms of life. Trisodium 2-hydroxy-1-(4-sulphonato-1-naphthylazo) naphthalene-3,6-disulphonate (Amaranth) is a hazardous dye which is widely used for coloring paper, textiles, phenol-formaldehyde resins, leather, and wood. It was also used as a food additive in jellies, jams, and cake decoration before being legally prohibited to be employed as a coloring agent for food and beverages. However, the carcinogenic nature of this dye is still debatable. It has also been proved that a higher concentration of Amaranth can cause a tumor, allergic and respiratory problems by affecting human/animal health adversely [2]. Evidence suggests that it can cause birth defects too [3]. Because of its high solubility, it is difficult to remove this water-soluble dye by common chemical treatments. Accordingly, an easy, feasible and reliable method is required for Amaranth removal. Various biological and physicochemical methods have been employed for removing dyes, such as adsorption, coagulation, precipitation, ion exchange, filtration, electrolysis and biological treatments [4]. Removal of dye using adsorption technique has recently attracted lots of attention due its efficiency, economic feasibiliy, simplicity of design, recycle of adsorbent, and no secondary pollution [5,6]. However, providing an efficient adsorbent for fundamental and practical applications of adsorption is a great challenge. Adsorption of a variety of dyes onto LDHs has been reported recently [7-10]. The anionic clay of layered double hydroxide (LDH) is generally expressed as $[M^{2+}_{1-x}M^{3+}_{x}(OH)_2]^{x+}[A^{n}_{x/n}]^{x-}\cdot mH_2O$, where M^{2+}, M^{3+} and A^{n-} represent trivalent metal cations, divalent metal cations, and interlayer anions, respectively [11], and x has been denoted

*Corresponding authors. E-mail: sohrabnas@pnu.ac.ir

as the molar ratio of M^{3+} to total metal [12]. LDH has exhibited its definite application in the adsorption of anions because of its layered structure, high surface area, high porosity, and interlayer anion mobility of its host A^{n-} [13]. Although dyes have a high adsorption capacity by LDHs, their industrial applications are still influenced by their low separation efficiency in aqueous solution. Meanwhile, magnetic separation technology has attracted much attention because of its easy separation procedure, and also high separation efficiency under an external magnetic field [14, 15]. Accordingly, to enhance separation and re-dispersion of adsorbent from aqueous solution, the combination of LDH and magnetic nanoparticle has been developed recently [16,17]. Investigation of a process by varying in the effective factors individually, do not show the effect of simultaneously changing of these factors. A Conventional technique for optimizing a multivariable system which usually defines one factor at a time needs to perform a number of experiments and it cannot show the relation effects between the variables on the process. This method is not only time consuming, but also requires doing some experiments for determining optimum levels, which are unreliable. Recently, lots of statistical experimental design methods have been employed in chemical process optimization. To achieve this aim, experimental design techniques are very useful tools because they provide statistical models, which are helpful in understanding the interactions among the optimized parameters. These methods involve mathematical models to design chemical processes and analyze the process results. One of the suitable methods utilized in many fields is response surface methodology (RSM). RSM is a collection of statistical and mathematical techniques being useful for improving, developing and optimizing process and evaluating the relative significance of several affecting factors even when the complex interactions are present. The main purpose of RSM is determining the optimum operational conditions for the system or determining a region which satisfies the operating specifications [18]. Application of this method was reported in several bio-compatible materials systems [19-26]. So, the goal of this study is to examine the feasibility of applying magnetic LDHs composite as an adsorbent for effective removal of Amaranth dye with quickly magnetic separation. The Fe_3O_4/ZnFe-LDH composite is prepared and their physical structure and chemical properties are characterized. The experimental design and response surface methodology (RSM) are also applied as the efficient approaches for establishing empirical models used for the prediction of adsorption processes.

EXPERIMENTS

Materials and Instrumentation

The Amaranth dye used in this research was supplied by Merck Company (Darmstadt, Germany). The stock solution (200 mg l^{-1}) of Amaranth was prepared, and working solution daily was prepared from its subsequent dilution. A digital pH meter (InoLab pH 730, Germany) was employed for adjusting pH. The scanning electron microscopy (SEM) was performed by a Hitachi, model S-4160. UV-Vis spectra were recorded on a V-670, JASCO spectrophotometer, and the BET analysis was performed using BELSORP Mini II instrument. FT-IR absorption spectra of AC were obtained using KBr disk by FT-IR (model 460 plus) in the region of 4000-400 cm^{-1}.

Preparation of Magnetic Layer Double Hydroxide (Fe_3O_4/ZnFe-LDH)

In a typical procedure, 0.2 g of cetyltrimethylammonium bromide was dissolved in 50 ml distilled water at 80 °C (Solution 1). For preparing solution 2, 10 mmol of $FeCl_3.6H_2O$, 5 mmol of $FeCl_2.4H_2O$ was dissolved in 50 ml distilled water. Then, solution 2 was added into solution 1 under constant stirring. Then, 15 ml of the NaOH 4 M solution was added drop wise into the above solution. After stirring the mixture for 2 h at room temperature, the precipitate was poured into the beaker to neutralize its pH. Finally, heat treatment of the product (Fe_3O_4) was carried out at 900 °C for 1 h. Then, 0.1 g of Fe_3O_4 was dispersed in 50 ml deionized water, with the pH adjusted to 10 (pH of the buffered solution for adjusting was obtained by dissolving 1.28 g Na_2CO_3 and 1.6 g NaOH in 100 ml of a 1:1 (v:v) methanol-water solution). Then, 20 ml aqueous solution containing 1.44 mmol $Zn(NO_3)_2.6H_2O$ and 0.48 mmol $Fe(NO_3)_3.9H_2O$ was added dropwise to the suspension of Fe_3O_4 under vigorous stirring and the solution pH maintained at 10. The solution was ultrasonicated for 1

h, and the products were collected and redispersed in 70 ml of deionized water for 1 h. The synthesized Fe_3O_4/ZnFe-LDH was collected from the reaction mixture by the external magnetic field and dried at 50 °C under vacuum.

Adsorption Studies

The dye concentrations were determined according to general traditional spectrophotometer method at its maximum wavelength over working concentration range. The efficiency of Amaranth removal was determined at different experimental conditions specified according to CCD method. The isotherm studies were investigated at Amaranth value in the range of 10-30 mg l^{-1} to obtain adsorption isotherms. The dyes removal percentages were calculated using the Eq. (1):

$$\%Amaranth\ \ removal = \frac{(C_0 - C_t)}{C_0} \times 100 \quad (1)$$

$$q_e = \frac{(C_0 - C_e)V}{W} \quad (2)$$

where C_0 (mg l^{-1}) and C_t (mg l^{-1}) are the concentrations of target at initial and after time t, respectively. The adsorbed dye amount (q_e (mg g^{-1})) was calculated by the Eq. (2): where C_0 and C_e (mg l^{-1}) are the initial and equilibrium dye concentrations in aqueous solution, respectively, V (l) is the volume of the solution, and W (g) is the mass of the adsorbent.

RESULTS AND DISCUSSION

Characterization

The FT-IR spectrum of ZnFe-LDH and magnetic Fe_3O_4/ZnFe-LDH was shown in Fig. 1. The υ (H-O-H) $_{Bending}$ and υ(O-H) $_{Sym}$ bands in this compound appeared in the ranges 1610-1630 cm^{-1} and 3440-3470 cm^{-1}, respectively. Also, ZnFe-LDH showed an intense band at 1384 cm^{-1} associated with the nitrate ion.

The SEM images of ZnFe-LDH and Fe_3O_4/ZnFe-LDH, shown in Fig. 2, were also studied. It is evident that the surface morphology of magnetic Fe_3O_4/ZnFe-LDH is different from that in ZnFe-LDH sample.

One of the most successful methods for gas adsorption onto a solid surface is the BET method. The adsorption method of Brunauer, Emmett, and Teller (BET) is based on the physical adsorption of a vapor or gas onto the surface of a solid. Such data can be used to analyse the porosity of the materials being studied. In this research, the BET method was used. The interference by the surrounding phase is especially problematic for the Bruner-Emmet-Teller (BET) N_2-adsorption/desorption isotherm because the entire surface is modified by the vacuum treatment before N_2-adsorption. The surface properties of adsorbent are presented in Table 1. According to the BET analysis, the specific surface area of Fe_3O_4/ZnFe-LDH was 1.6324×10^2 m^2 g^{-1}, which is larger than ZnFe-LDH. Also, the total pore volume and the average pore diameter of Fe_3O_4/ZnFe-LDH were 0.64 cm^3 g^{-1} and 15.7 nm. Figure 3 shows the EDS spectrum of the prepared sample which confirms the presence of relevant elements and the purity of the synthesized Fe_3O_4/ZnFe-LDH.

Response Surface Methodology

Response surface methodology (RSM) has been used to optimize five variables; the initial concentration of Amaranth, pH, adsorbent dosage, temperature and contact time. These five variables were chosen as independent variables. The amount of Amaranth removed (mg g^{-1}) was set as the output response variable. The ranges and levels of the variables are shown in Table 2. Design Expert V.7.1.5 software was used for response surface modeling, statistical analysis, and optimization. The combined effect of those three variables was investigated using central composite design (CCD). The 32 sets of experiments including six replications in Table 3 were performed. The data were analyzed using analysis of variance (ANOVA) and the optimal values of the Amaranth removal were estimated using the 3D response surface analysis of the variable.

Central Composite Design (CCD)

As showed in Table 2, five independent variables were studied into three levels (low, basal and high) with coded value (+1, 0, -1) and the star points of +2 and -2 for +α and -α, respectively, were selected for each set of experiments. This method along with an analysis of variance (ANOVA) is used to investigate the main interaction and quadratic effects of all variables.

A p-value less than 0.05 in the anova table shows the statistical importance of an effect at 95% confidence level.

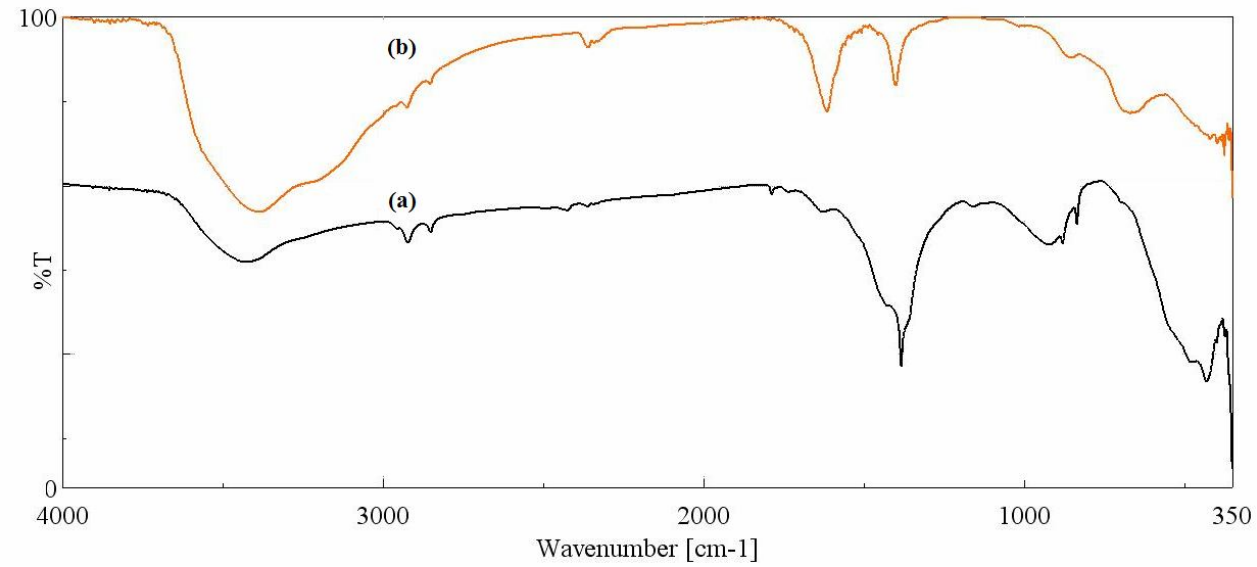

Fig. 1. The FT-IR spectra of (a) ZnFe-LDH, and (b) Fe_3O_4/ZnFe-LDH.

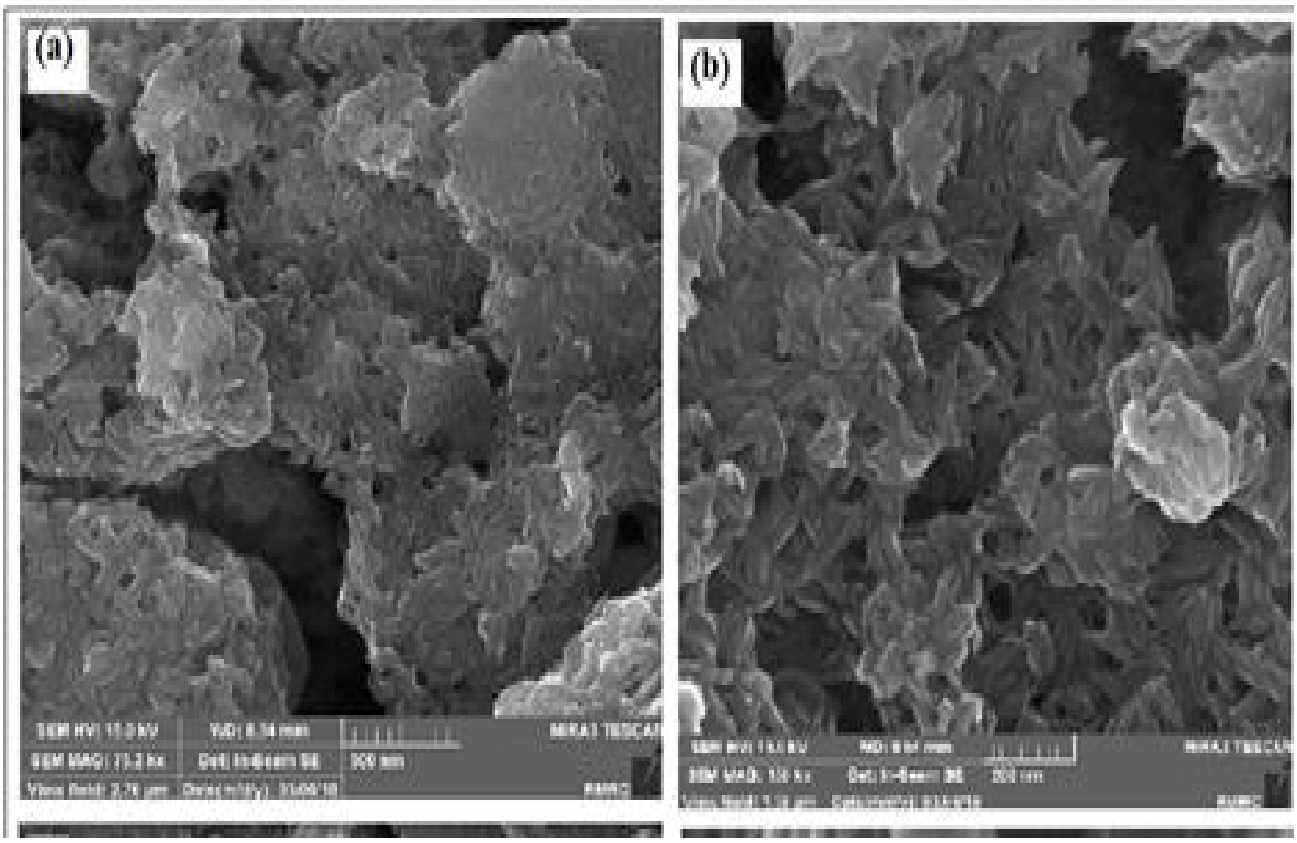

Fig. 2. The SEM images of (a) ZnFe-LDH and (b) Fe_3O_4/ZnFe-LDH.

Table 1. The Results of Surface Area and Porosity Measurement (BET Method) for ZnFe-LDH and Fe_3O_4/ZnFe-LDH

Sample	Surface area ($m^2\ g^{-1}$)	Micropore Vol. ($cm^3\ g^{-1}$)	Micropore size (nm)
Fe_3O_4/ZnFe-LDH	1.6324×10^2	0.64	15.7
ZnFe-LDH	60	0.3	22

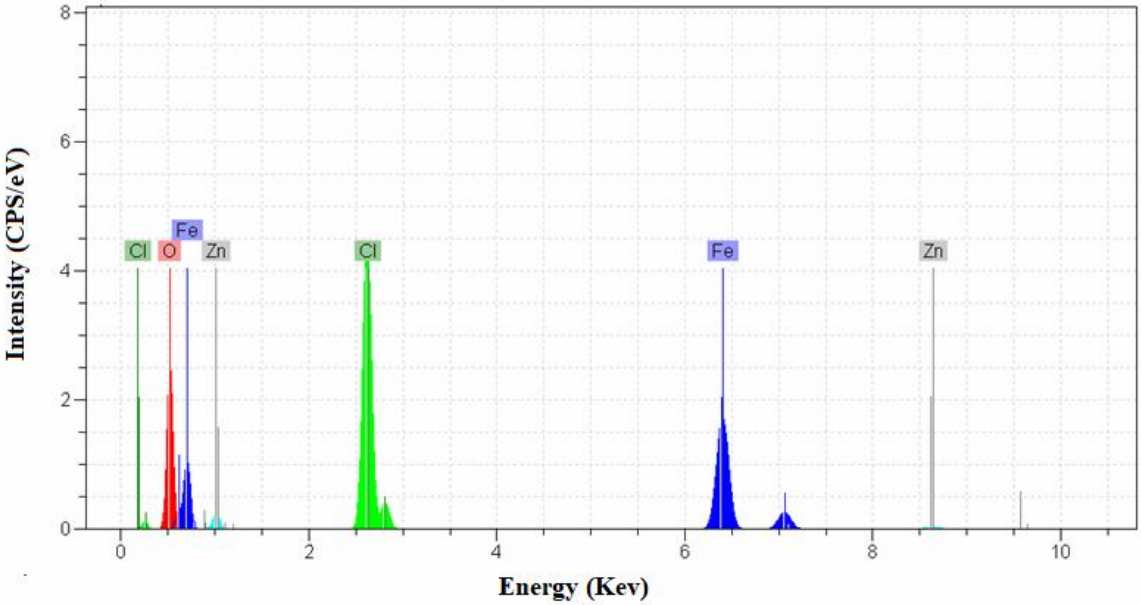

Fig. 3. The EDS spectrum of the synthesized Fe3O4/ZnFe-LDH.

Table 2. Experimental Factors and Levels in the Central Composite Design

			Levels				
Factors	Unit	Symbol	-α	Low (-1)	Central (0)	High (+1)	+α
Concentration	$mg\ l^{-1}$	A	10	27.5	45	62.5	80
pH		B	2	2.75	3.5	4.25	5
Adsorbent dosage	mg	C	0.01	0.07	0.13	0.19	0.25
Temperature	°C	D	25	28.75	32.5	36.25	40
Contact time	Min	E	15	22.5	30	37.5	45

Table 3. Central Composite Design (CCD) with Variables, Observed and Predicted Values for Removal Efficiency (%) of Amaranth

Std. order	Run order	Blocks	Initial concentration	pH	Adsorbent dosage	Temperature	Contact time	Response
13	1	1	10	2	0.25	40	45	69.8
29	2	1	45	3.5	0.13	32.5	30	91.13
26	3	1	45	3.5	0.13	32.5	60	91.1
32	4	1	45	3.5	0.13	32.5	30	91
5	5	1	10	2	0.25	25	15	65.59
11	6	1	10	5	0.01	40	45	99.67
25	7	1	45	3.5	0.13	32.5	60	91.19
15	8	1	10	5	0.25	40	15	93.74
8	9	1	80	5	0.25	25	15	92.95
4	10	1	80	5	0.01	25	45	*99.98*
27	11	1	45	3.5	0.13	32.5	30	85.42
1	12	1	10	2	0.01	25	45	99.83
10	13	1	80	2	0.01	40	45	99.97
19	14	1	45	4	0.13	32.5	30	91.17
31	15	1	45	3.5	0.13	32.5	30	87.24
28	16	1	45	3.5	0.13	32.5	30	*97.6*
23	17	1	45	3.5	0.13	17.5	30	*97.07*
6	18	1	80	2	0.25	25	45	94.13
9	19	1	10	2	0.01	40	15	99.32
22	20	1	45	3.5	0.37	32.5	30	95.64
24	21	1	45	3.5	0.13	47.5	30	*99.76*
20	22	1	45	6.5	0.13	32.5	30	97.73
12	23	1	80	5	0.01	40	15	99.95
30	24	1	45	3.5	0.13	32.5	30	96.04
17	25	1	25	3.5	0.13	32.5	30	*99.52*
16	26	1	80	5	0.25	40	45	94.87
14	27	1	80	2	0.25	40	15	99.35
3	28	1	10	5	0.01	25	15	*99.77*
21	29	1	45	3.5	0.11	32.5	30	*97.71*
18	30	1	15	3.5	0.13	32.5	30	93.13
2	31	1	80	2	0.01	25	15	*99.99*
7	32	1	10	5	0.25	25	45	93.67

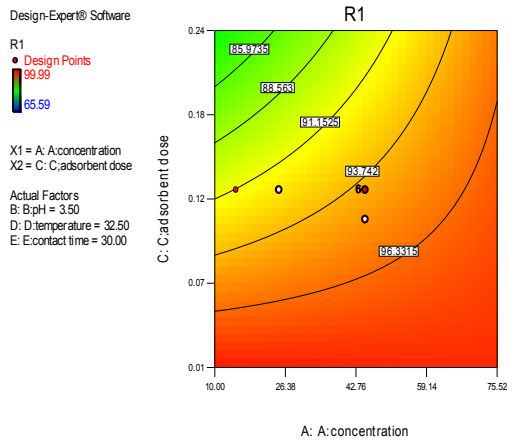

a

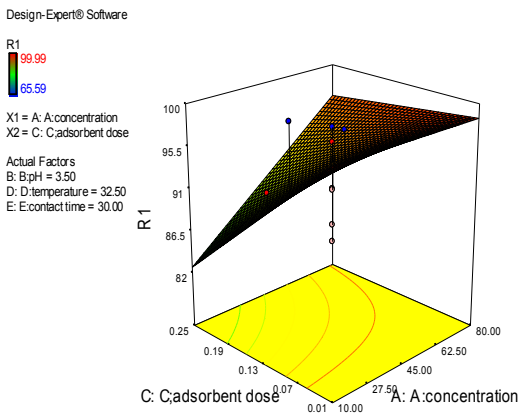

b

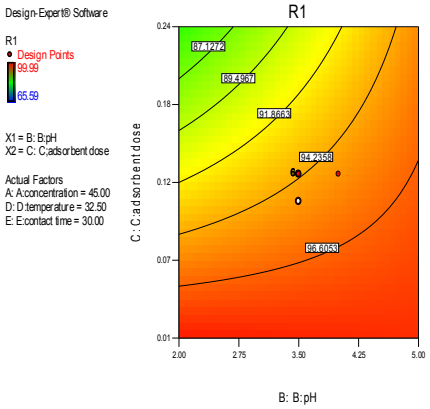

c

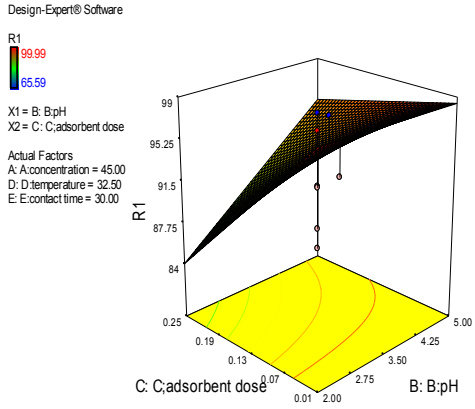

d

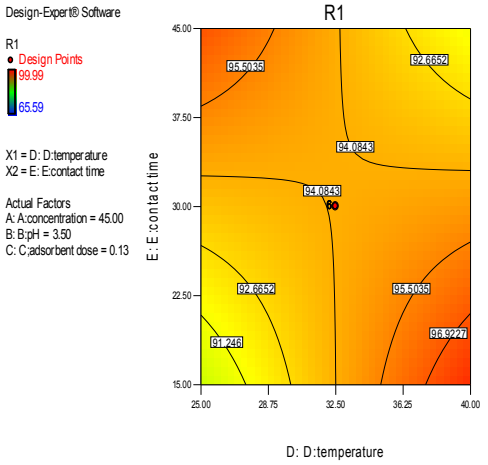

e

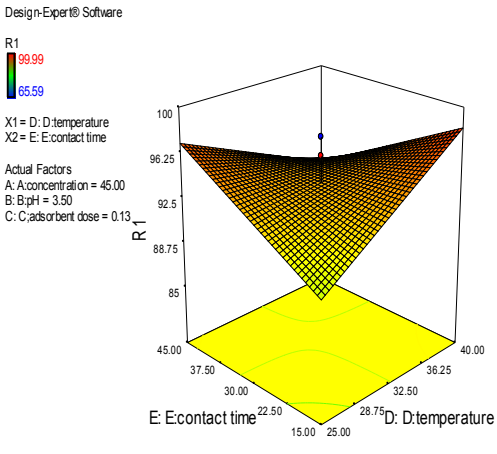

f

Fig. 4. 3D surface and contour plots for interactive effect variables.

F-test was used to evaluate the statistical significance of each term in the polynomial equation whithin 95% confidence interval. Data analysis gave a semi-emperical experssion of extraction recovery (ER%) with the following equation.

The analysis of data gave the semi-empirical expression wrote as:

$$y = +93.46 + 3.23A + 3.03B - 5.76C + 0.67D + .045E - 3.62AB + 3.58AC + 0.21AD - 0.49AE + 2.88BC - 0.46BD + .14BE + 0.76CD + 0.026CE - 3.59DE - 1.79A2 - .82B2 + 3.09C2 + 1.07D2 - 0.75E2$$

where, y is the amount of Amaranth (mg g^{-1}), A is the initial concentration of Amaranth (mg l^{-1}), B is pH, C is adsorbent dosage (mg), D is temperature (°C) and, E is contact time (min).

The acceptable quality of polynomial model fit expressed with the coefficient of determination value (R^2 = 0.9922 and adjusted R^2 = 0.9427). The plot of experimental removal percentage *versus* calculated value indicates a good fit (Fig. 5).

Equilibrium Isotherms Models

The experimental results from adsorption of Amaranth dye on the magnetic Fe_3O_4/ZnFe-LDH were analyzed by Langmuir, Freundlich and Tempkin models. The Langmuir isotherm can be considered as Eq. (3) [27]:

$$C_e/q_e = 1/q_{max}K_L + C_e/q_{max} \quad (3)$$

where q_e (mg g^{-1}) and C_e (mg l^{-1}) are the amounts of adsorbed dye per unit mass of adsorbent and unadsorbed dye concentration in solution at equilibrium, respectively. The q_{max} is the maximum amount of the Amaranth dye per unit mass of adsorbent on the surface bound at high C_e (mg g^{-1}), and K_L is adsorption equilibrium constant (l mg^{-1}). Fig. 6a shows the linear plot of C_e/q_e *vs.* C_e of Langmuir isotherm. The values of q_{max} and K_L were determined from slope and intercepts of the plots and are presented in Table 5.

The Freundlich's adsorption isotherm model can be applied for a multilayer heterogeneous adsorption and expressed as Eq. (4) [28]:

$$\log q_e = 1/n\log C_e + \log K_F \quad (4)$$

where K_F (l g^{-1}) is the Freundlich isotherm constants related to the maximum adsorption capacity and n is the intensity of adsorption. Figure 6b shows the linear plot of ($\log q_e$ *vs.* $\log C_e$) of Freundlich isotherm. The plot of $\log q_e$ *vs.* $\log C_e$ was employed to generate the intercept value of K_F and the slope of $1/n_F$ (Table 4).

The heat of the adsorption and the interaction of adsorbent-adsorbate were studied using Tempkin isotherm model as expressed in Eq. (5) [29]:

$$q_e = B_t\ln K_T + B_t\ln C_e \quad (5)$$

in this model, B_t is the Tempkim constant related to the heat of adsorption (J mol^{-1}), T is the absolute temperature (K), and K_T is the equilibrium binding constant (l mg^{-1}). Figure 6c shows the linear plot of q_e *vs.* $\ln C_e$ of Tempkim isotherm model.

The constant parameters of isotherm equations and the correlation coefficient (R^2) for isotherm models are summarized in Table 5. The high correlation coefficient at various conditions shows the applicability of Tempkin model for investigation of the experimental data.

Adsorption Kinetics

The kinetic analysis based on the kinetic models including pseudo first- and second-order, Elovich and intraparticle diffusion (Figs. 7a-d) give good knowledge about the rate and mechanism of adsorption. Table 6 summarizes the obtained results of each model. The highest R^2 value of this model (1.0000) confirm the applicability of this model to interpret the experimental data.

Thermodynamic Study

In order to describe the thermodynamic adsorption behavior of Amaranth onto Fe_3O_4/ZnFe-LDH, thermodynamic parameters were calculated including the change in free energy (ΔG°), enthalpy (ΔH°) and entropy (ΔS°) using the following thermodynamic equations (Table 7) [30]:

$$\Delta G° = -RT\ln K_c \quad (6)$$

Table 4. Summary of Statistical Models

Source	Std. Dev.	R-squared	Adjusted R-squared	Predicted R-squared	Press	
Linear	6.83	0.3870	0.2691	0.0363	2047.53	
2FI	5.25	0.7769	0.5677	-0.8407	3636.79	
Quadratic	1.5	0.9922	0.9427	0.8695	554.28	Suggested

Table 5. ANOVA for Response Surface Quadratic Model of Fe_3O_4/ZnFe-LDH

Source	Sum of squares	df	Mean square	F Value	p-value	
Model	1717.92	20	85.90	3.66	0.0155	Significant
A	175.04	1	175.04	7.47	0.0195	
B	148.44	1	148.44	6.33	0.0287	
C	536.42	1	536.42	22.88	0.0006	
D	10.85	1	10.85	0.46	0.5103	
E	0.049	1	0.049	2.073E-003	0.9645	
AB	210.25	1	210.25	8.97	0.0122	
AC	204.49	1	204.49	8.72	0.0131	
AD	0.73	1	0.73	0.031	0.8630	
AE	3.84	1	3.84	0.016	0.6934	
BC	132.83	1	132.83	5.67	0.0365	
BD	3.10	1	3.10	0.13	0.7231	
BE	0.33	1	0.33	0.014	0.9076	
CD	9.12	1	9.12	0.39	0.5455	
CE	0.011	1	0.011	4.703E-004	0.9831	
DE	205.64	1	205.64	8.77	0.0129	
A^2	12.98	1	12.98	0.55	0.4723	
B^2	8.48	1	8.48	0.36	0.5597	
C^2	121.02	1	121.02	5.16	0.0441	
D^2	31.63	1	31.63	1.35	0.2700	
E^2	15.69	1	15.69	0.67	0.4307	
Residual	257.85	11	23.44			
Lack of fit	144.58	6	24.10	1.06	0.4831	Not significant
Pure error	113.27	5	22.65			
Cor total	1975.77	31				
Adeq	8.705					

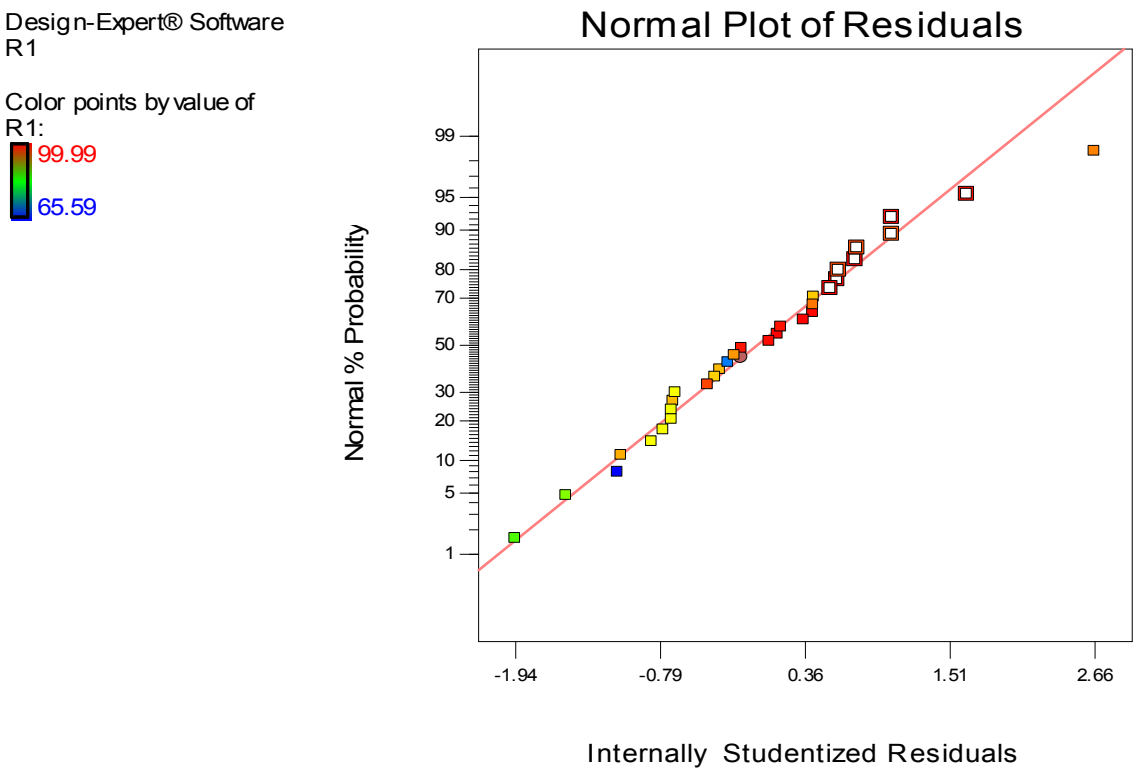

Fig. 5. The plot of the experimental removal percentage *versus* the calculated value.

Table 5. Isotherm Constant Parameters and Correlation Coefficients Calculated for the Adsorption of Amaranth onto Fe_3O_4/ZnFe-LDH

Isotherms	Equation	Parameters	Value
Langmuir	$\frac{C_e}{q_e} = \frac{1}{K_1 q_m} + \frac{C_e}{q_m}$	q_m (mg g^{-1})	42.55
		K_L (l mg^{-1})	1.5460
		R^2	0.9669
Freundlich	$\ln q_e = \ln K_f + \frac{1}{n} \ln C_e$	1/n	0.3791
		K_f (mg g^{-1}) (l mg^{-1})$^{1/n}$	0.1302
		R^2	0.9618
Tempkin	$q_e = B_t \ln K_T + B_t \ln C_e$	Bt	116.52
		K_T (l mg^{-1})	0.7461
		R^2	0.9750

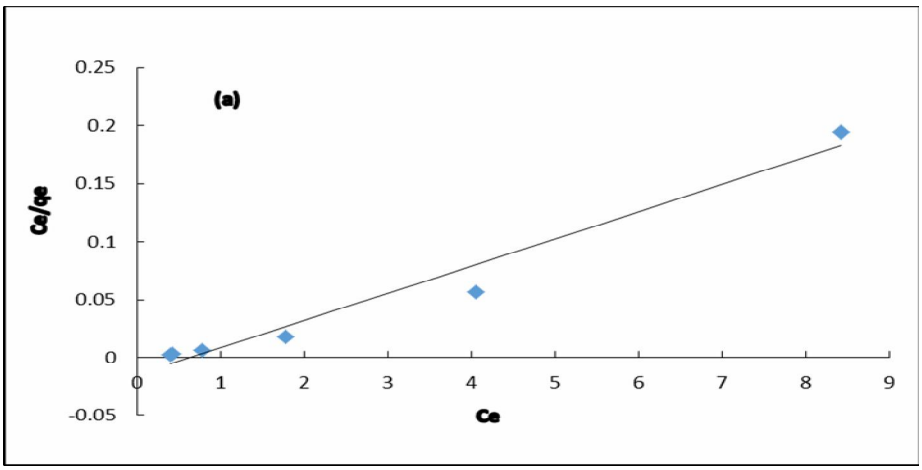

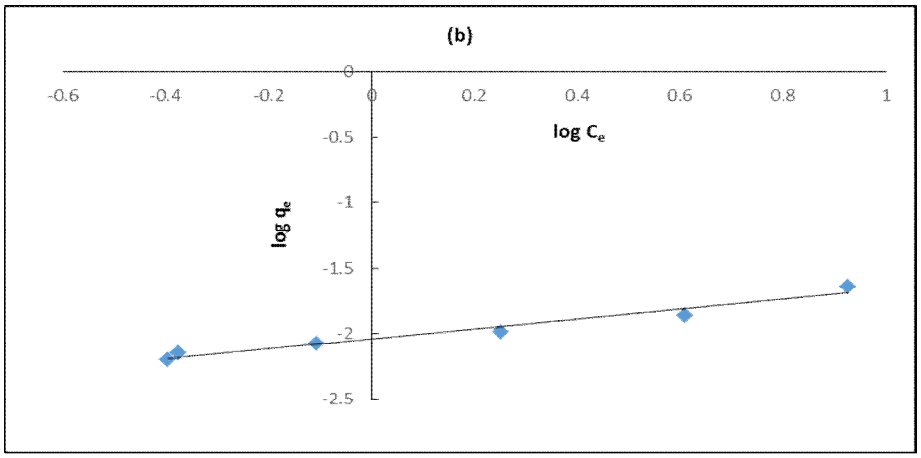

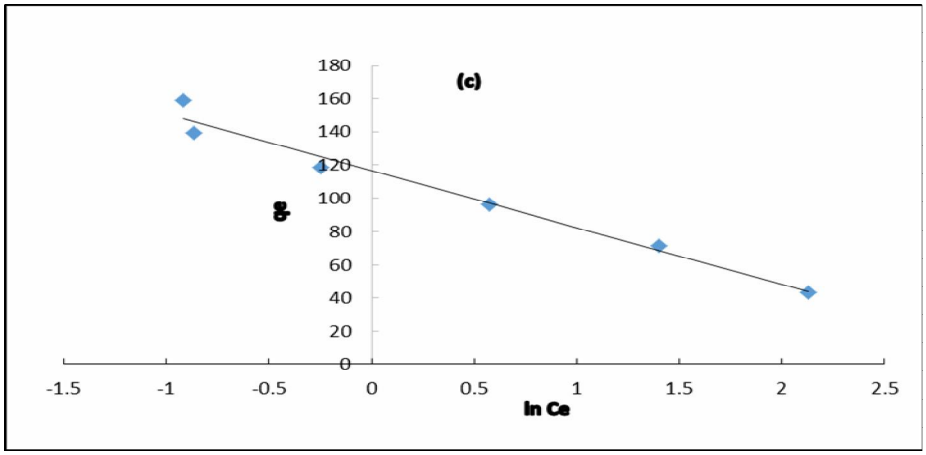

Fig. 6. The plot of (a) Langmuir equilibrium isotherm, (b) Freundlich isotherm and (c) Tempkin isotherm.

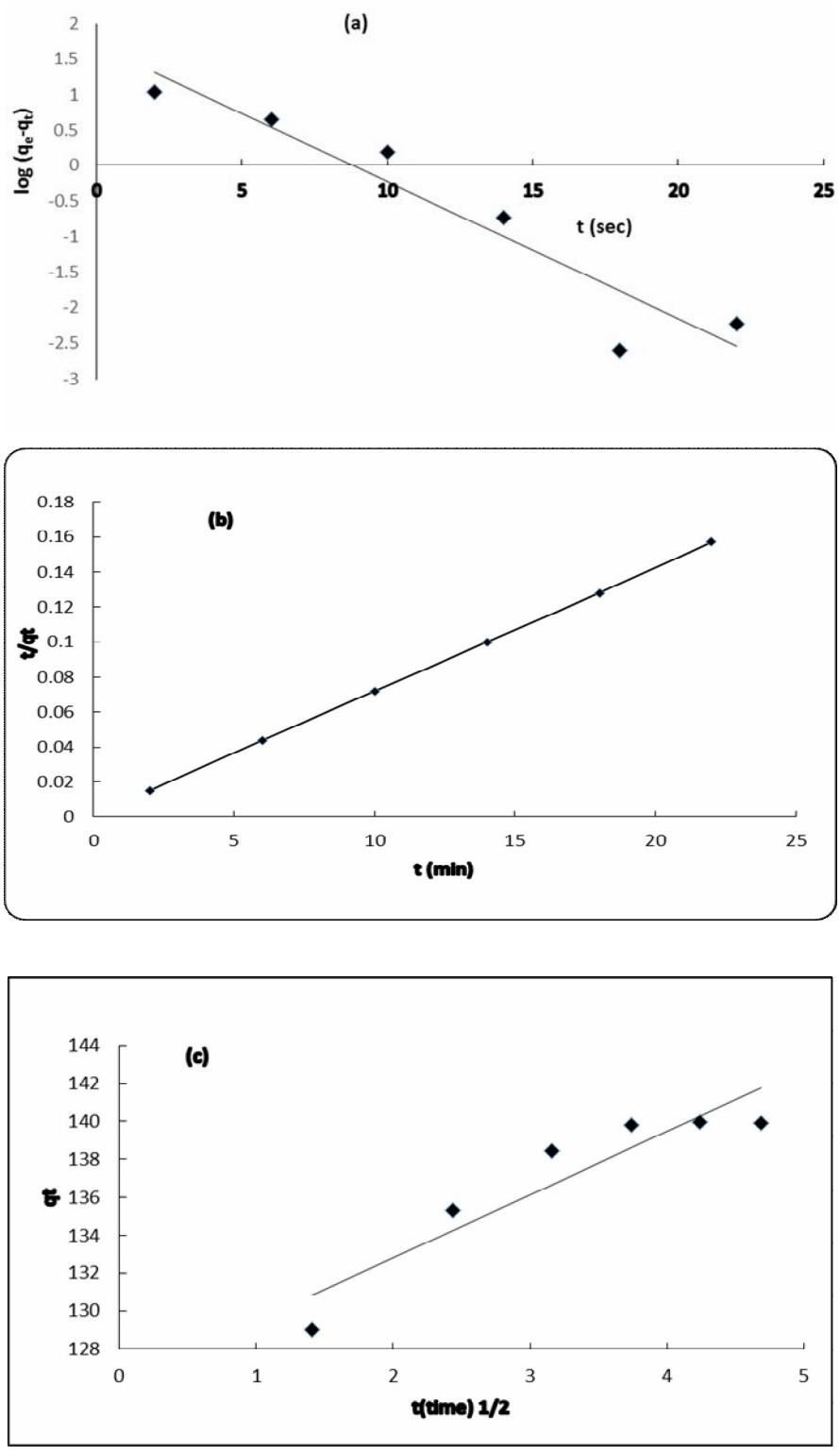

Fig. 7. Linear plot of the (a) pseudo-first order kinetic, (b) pseudo-second-order kinetic, (c) intra-particle diffusion kinetic and (d) Elovich kinetic.

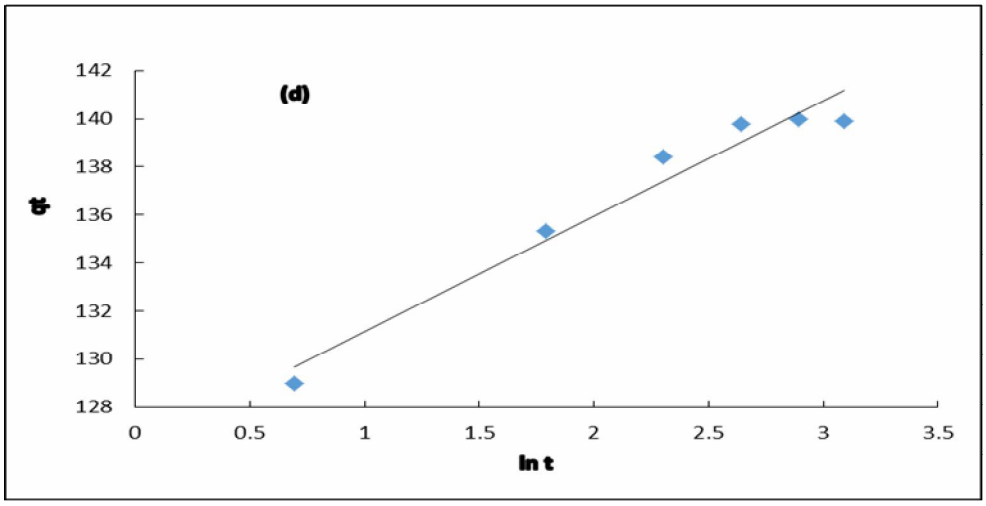

Fig. 7. Continued.

Table 7. The Thermodynamic Parameters for Sorption of Amaranth at Different Temperatures

Thermodynamic parameters	Values (kJ mol^{-1})
-Δ*H*°	56.30
-Δ*S*°	10.62
-Δ*G*°	15.17
lnK_c	5.98

$$\ln K_c = \Delta S°/R - \Delta H°/RT \quad (7)$$

where R is the universal gas constant (8.314 J K^{-1} mol^{-1}), T is the absolute solution temperature (K), and K_c represents the equilibrium adsorption constant.

The plots of lnK_c *vs*. 1/T give the straight line from which ΔH° and ΔS° are calculated from the slope and intercept, respectively (Fig. 8).

The negative values of ΔG° indicate that the adsorption process was spontaneous and feasible at all the studied temperatures. Moreover, the negative value of ΔH° (-56.30 kJ mol^{-1}) indicates that adsorption followed an exothermic process. The negative value of ΔS° (-10.62 kJ mol^{-1}) also suggests decreased randomness at the solid-solution interface during the adsorption process. Table 8 gives a comparison of the present study with some reported result in terms of adsorption capacity results. The result showed its superiority to the reported literature.

Determination of Zero Ppoint Charge

Determination of point of zero charge (pHz) was done to determine the surface charge (or the stability) of Fe3O4/ZnFe-LDH. For the determination of pHz, 0.1 M NaCl was prepared, and its initial pH was adjusted between 2.0 and 12.0 using HCl and NaOH. Then, 20 ml of 0.1 M NaCl was taken in 25 ml flasks and 0.05 g of Fe_3O_4/ZnFe-

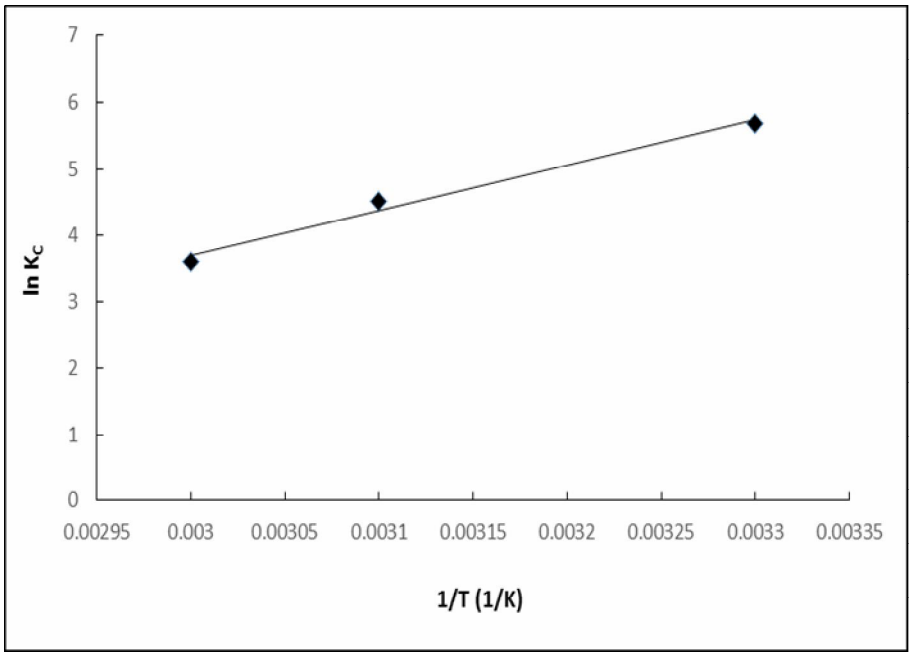

Fig. 8. The plots of lnK_c *vs*. 1/T.

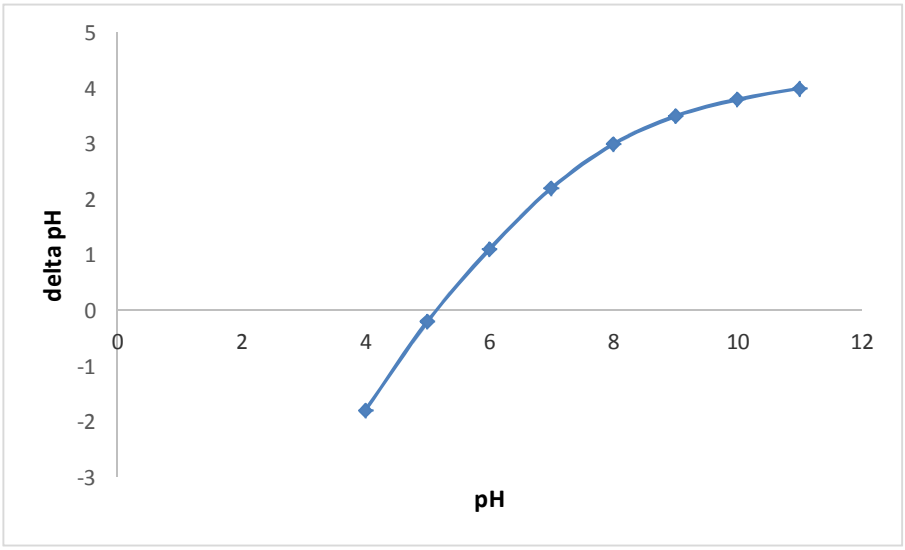

Fig. 9. Zero point charge determination.

LDH was added to each solution. These flasks were kept for 24 h and the final pH of the solutions was measured with a pH meter. Graphs were plotted between final pH and initial pH. From Fig. 9, it is clear that at 5.1, delta pH is zero, therefore, the pHz of Fe_3O_4/ZnFe-LDH is 5.1.

Reusibility of the Fe_3O_4/ZnFe-LDH

The ability of reusing the adsorbents in several

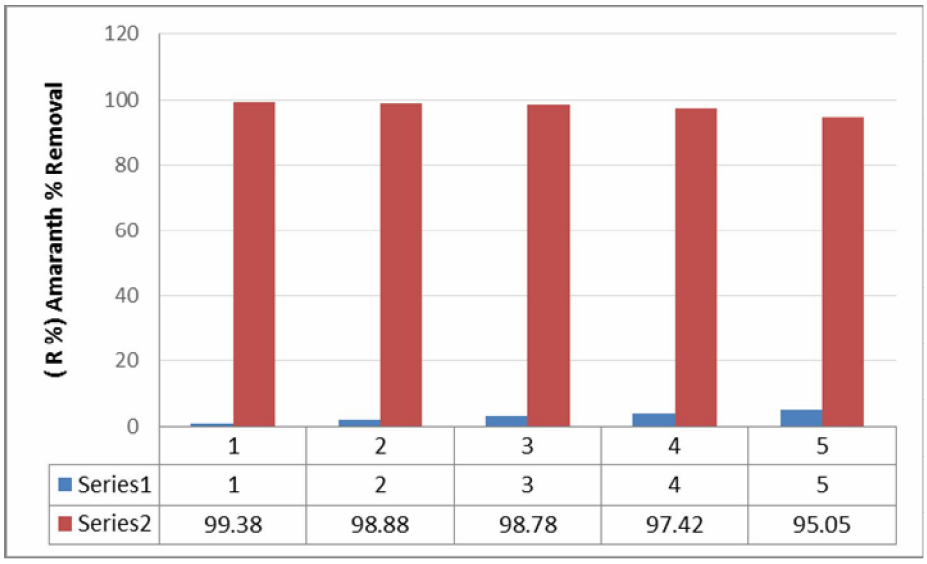

Fig. 10. The ability of reusing Fe_3O_4/ZnFe-LDH in five successive separation processes.

Table 8. Comparison of the Amaranth Removal in Different Methods and Adsorbents

Adsorbent	q_e (mg g^{-1})	Ref.
Supported nano-FeOOH	0.228	[31]
Iron oxide magnetic nanoparticles (IOMN)	1.050	[32]
Alumina reinforced polystyrene (ARBA)	7.8360	[33]
Bottom ash	0.7860	[34]
De-oiled soya	0.1288	[34]
Fe_3O_4/ZnFe-LDH	42.550	This work

successive separation processes was examined. The obtained results showed that Fe_3O_4/ZnFe-LDH can be reused for five times without any decrease in their efficiency.

Comparision with other Studies

Table 8 gives a comparison of present study with some previously reported results in term of adsorption capacity .The result shows its superiority to those reported in the literature [31-34].

CONCLUSIONS

The objective of the present study was to find out the optimum condition to maximize the adsorption of Amaranth by developing a model equation. The response surface modeling based on five variables of central composite design was used to determine the individual as well as the combined effect of different reaction variables such as the initial concentration of Amaranth, pH, adsorbent dosage, temperature, and contact time. The regression analysis and

optimization of variables were carried out using design expert software for predicting the response in all experimental regions. The experimental values were found to be in well agreement with the predicted values from the model. The optimum production condition was found to be initial Amaranth concentration of 70.93 mg l^{-1}, a pH value of 3.6, adsorbent dosage of 0.01 g, the temperature of 31.82 °C, and contact time of 16.83 min.

ACKNOWLEDGEMENTS

The financial support of the research council of the Payame Noor University of Isfahan is gratefully acknowledged.

REFERENCES

[1] Lawal, I. A.; Moodley, B., Synthesis, characterisation and application of imidazolium based ionic liquid modified montmorillonite sorbents for the removal of amaranth dye. *RSC Adv.,* **2015**, *5*, 61913-61924, DOI: 10.1039/C5RA09483F.

[2] Ahmad, R.; Kumar, R., Adsorption of amaranth dye onto alumina reinforced polystyrene clean-soil, air, water, **2011**, *39*, 74-82, DOI: 10.1002/ clen.201000125.

[3] Talmage, D.; Biologic Markers in Immunotoxicology, The National Academies Press, Washington DC, 1992, p. 37.

[4] Robinson, T.; McMullan, G.; Marchant, R.; Nigam, P., Remediation of dyes in textile effluent: a critical review on current treatment technologies with a proposed alternative. *Biores. Technol.* **2001**, *77*, 247-255, DOI: 10.1016/S0960-8524(00)00080-8.

[5] Rouquerol, J.; Rouquerol, F.; Llewellyn, P.; Maurin, G.; Sing, K., Adsorption by powders and porous solids, 2th Ed., Academic Press, Amsterdam, 2014.

[6] Do, D. D., Adsorption Science and Technology: Proceedings of the Second Pacific Basin Conference on Adsorption Science and Technology, World Scientific, Brisbane, 2000.

[7] Aguiar, J. E.; Bezerra, B. T. C.; Braga, B. D.; Lima, P. D. D.; Nogueira, R. E. F. Q.; de Lucena, S. M. P.; da Silva, I. J., Adsorption of anionic and cationic dyes from aqueous solution on non-calcined Mg-Al layered double hydroxide:an experimental and theoretical study. *Sep. Sc. Technol.* **2013**, *48*, 2307-2316, DOI: 10.1080/01496395.2013.804837.

[8] Extremera, R.; Pavlovic, I., Perez, M. R.; Barriga, C., Removal of acid orange 10 by calcined Mg/Al layered double hydroxides from water and recovery of the adsorbed dye. *Chem. Eng. J.* **2012**, *213*, 392-400, DOI: 10.1016/j.cej.2012.10.042.

[9] Dos Santos, R. M. M.; Gonçalves, R. G. L.; Constantino, V. R. L.; da Costa, L. M.; da Silva, L. H. M.; Tronto, J.; Pinto, F. G., Removal of acid green 68:1 from aqueous solutions by calcined and uncalcined layered double hydroxides. *Appl. Clay Sci.* **2013**, *80*,189-195, DOI: 10.1016/ j.clay.2013.04.006.

[10] Bouhent, M. M.; Derriche, Z.; Denoyel, R.; Prevot, V.; Forano, C., Thermodynamical and structural insights of orange II adsorption by $MgRAlNO_3$ layered double hydroxides. *J. Solid State Chem.* **2011**, *184*, 1016-1024, DOI: 10.1016/j.jssc.2011.03.018.

[11] Woo, M. A.; Kim, T. W.; Paek, M. J.; Ha, H. W.; Choy, J. H.; Hwang, S. J., Phosphate-intercalated Ca-Fe-layered double hydroxides: Crystal structure, bonding character, and release kinetics of phosphate. *J. Solid State Chem.* **2011**, *184*, 171-176, DOI: 10.1016/j.jssc.2010.11.003.

[12] Wang, L.; Xu, X.; Evans, D. G.; Duan, X.; Li, D., Synthesis and selective IR absorption properties of iminodiacetic-acid intercalated MgAl-layered double hydroxide. *J. Solid State Chem.* **2010**, *183*, 1114-1119, DOI: 10.1016/j.jssc.2010.03.022.

[13] Baliarsingh, N.; Parida, K. M.; Pradhan, G. C., Influence of the nature and concentration of precursor metal ions in the brucite layer of LDHs for phosphate adsorption - a review. *RSC Adv.* **2013**, *3*, 23865-23878, DOI: 10.1039/c3ra42857e.

[14] Ambashta, R. D.; Sillanpää, M., Water purification using magnetic assistance: A review. *J. Hazard. Mater.* **2010**, *180*, 38-49, DOI: 10.1016/ j.jhazmat.2010.04.105.

[15] Zaidi, N. S.; Sohaili, J.; Muda, K.; Sillanpaa, M., Magnetic field application and its potential in water and wastewater treatment systems, *Sep. Purif. Rev.* **2014**, *43*, 206-240, DOI: 10.1080/

15422119.2013.794148.

[16] Zhang, X.; Wang, J.; Li, R.; Dai, Q.; Gao, R.; Liu, Q.; Zhang, M., Preparation of Fe_3O_4@C@layered double hydroxide composite for magnetic separation of uranium. *Ind. Eng. Chem. Res.* **2013**, *52*, 10152-10159, DOI: 10.1021/ie3024438.

[17] Chen, C. P.; Gunawan, P.; Xu, R., Self-assembled Fe3O4-layered double hydroxide colloidal nanohybrids with excellent performance for treatment of organic dyes in water. *J. Mater. Chem.* **2011**, *21*, 1218-1225, DOI: 10.1039/C0JM01696A.

[18] Mahalik, K.; Sahu, J. N.; Patwardhan, A.; Meikap, B. C., Statistical modeling and optimization of hydrolysis of urea to generate ammonia for flue gas conditioning. *J. Hazard. Mater.* **2010**, *182*, 603-610, DOI: 10.1016/j.jhazmat.2010.06.075.

[19] Arabi, M.; Ghaedi, M.; Ostovan, A., Development of a lower toxic approach based on green synthesis of water-compatible molecularly imprinted nanoparticles for the extraction of hydrochlorothiazide from human urine ACS sustainable. *Chem. Eng.* **2017**, *5*, 3775-3785, DOI:10.1021/acssuschemeng.6b02615.

[20] Ostovan, A.; Ghaedi, M.; Arabi, M.; Yang, Q.; Li, J.; Chen, L., Hydrophilic multi-template molecularly imprinted biopolymers based on a green synthesis strategy for determination of B-family vitamins. *Interfaces*, **2018**, *10*, 4140-4150, DOI: 10.1021/acsami.7b17500.

[21] Ostovan, A.; Ghaedi, M.; Arabi, M., Fabrication of water-compatible superparamagnetic molecularly imprinted biopolymer for clean separation of baclofen from bio-fluid samples: a mild and green approach. *Talanta*, **2018**, *7*, 179, 76, 768, DOI: 10.1016/j.talanta.2017.12.017.

[22] Ostovan, A.; Ghaedi, M.; Arabi, M.; Asfaram, A., Hollow porous molecularly imprinted polymer for highly selectiveclean-up followed by influential preconcentration of ultra-traceglibenclamide from bio-fluid, *J. Chromatography A* **2017**, *1530*, 65-74, DOI: 10.1016/j.chroma.2017.09.026.

[23] Novel strategy for synthesis of magnetic dummy molecularly imprinted nanoparticles based on functionalized silica as an efficient sorbent for the determination of acrylamide in potato chips: optimization by experimental design methodology, *Talanta*, **2016**, *1*, 154, 526-3210, DOI: 10.1016/j.talanta.2016.04.010.

[24] Development of dummy molecularly imprinted based on functionalized silica nanoparticles for determination of acrylamide in processed food by matrix solid phase dispersion, *Food Chem.* **2016**, *1*, 210, 78-84, DOI: 10.1016/j.foodchem.2016.04.080.

[25] Water compatible molecularly imprinted nanoparticles as a restricted access material for extraction of hippuric acid,a biological indicator of toluene exposure, from human urine *Microchimica Acta,* **2017**, *184*, DOI: 10.1007/s00604-016-2063-5.

[26] Synthesis and application of *in-situ* molecularly imprinted silica monolithic in pipette-tip solid-phase microextraction for the separation and determination of gallic acid in orange juice samples new. *J. Chem.,* **2017**, *41*, 3308, DOI: 10.1016/j.jchromb.2017.02.016.

[27] Kannan, N.; Sundaram, M. M., Kinetics and mechanism of removal of methylene blue by adsorption on various carbone: A comparative study. *Dyes Pigm.* **2001**, *51*, 25-40, DOI: 10.1016/S0143-7208(01)00056-0..

[28] Citak D.; Tuzen M.; Soylak M., Simultaneous coprecipitation of lead, cobalt, copper, cadmium, iron and nickel in food samples with zirconium(IV) hydroxide prior to their flame atomic absorption spectrometric determination. *Food and Chem. Toxicol.* **2009**, *47*, 9, 2302-2307, DOI: 10.1016/j.fct.2009.06.021.

[29] Tempkin, M. J.; Pyzhev, V., Kinetics of ammonia synthesis on promoted iron catalysts. *Acta Physiochim.* U.S.S.R. **1940**, 12, 217-222, DOI: 10.1021/j100120a035 I.

[30] Nandi, B. K.; Goswami, A.; Purkait, M. K., Adsorption characteristics of brilliant green dye on kaolin. *J. Hazard. Mater.* **2009**, *161*, 387-395, DOI: 10.1016/j.jhazmat.2008.03.110.

[31] Guoquan Zhang, G.; Wang, S.; Yang, F., Efficient adsorption and combined heterogeneous/homogeneous fenton oxidation of amaranth using supported nano-FeOOH as cathodic catalysts. *J. Phys. Chem. C.* **2012**, *116*, 5, 3623-3634, DOI: 10.1021/jp210167b.

[32] Gutierre, A. M.; Dziubla, T. D., Recent advances on iron oxide magnetic nanoparticles as sorbents of organic pollutants in water and wastewater treatment. *Rev. Environ. Health*. **2017**, *32*, DOI: 10.1515/reveh-2016-0063.

[33] Ahmad, R.; Kumar, R., Adsorption of amaranth dye onto alumina reinforced polystyrene clean-soil, *Air, Water*. **2011**, *39*, 74-82, DOI: 10.1002/clen.201000125.

[34] Mittala A.; Lisha Kurup (Krishnan) L.; Gupta V. K., Use of waste materials-bottom ash and de-oiled soya, as potential adsorbents for the removal of amaranth from aqueous solutions *J. Hazard Mater. B,* **2005**, *117*, 171-178, DOI:10.1016/j.jhazmat.2004.09.016.